Advancing Fire Severity Analysis: Object-Based Image Classification with Landsat 8 on Kangaroo Island

Jiyu Liu,[1] Dr David Freudenberger,[2] and Associate Professor Samsung Lim,[1]

[1] School of Civil and Environmental Engineering, Faculty of Engineering, The University of New South Wales, NSW
[2] Fenner School of Environment & Society, College of Science, The Australian National University, ACT

Mapping burned areas and land-uses in Kangaroo Island using an object-based image classification framework and Landsat 8 Imagery from Google Earth Engine

This study integrates a multi-resolution segmentation method and a hierarchical classification framework to classify burned areas in Kangaroo Island, South Australia. Demonstrating the efficacy of an object-based image classification approach combining color and shape features, we show that objects segmented from multi-source data result in higher classification accuracy.

Introduction

Variations in spectral reflectance, particularly in Near-infrared (NIR) and short-wave infrared (SWIR) spectra, enable the determination of forest cover loss post-fire events using remote sensing techniques.

Pixel-based image analysis struggles to interpret landscape texture, structure, and shape information from optical images, leading to "salt and pepper noise" and reduced classification accuracy. Conversely, object-based image analysis segments images into smaller, real-world objects using color, shape, and topological features, allowing for more accurate fire severity level analysis. It integrates various spatial and contextual attributes into the mapping process, thereby enhancing mapping accuracy.

Methodology

Study area

Kangaroo Island (36°05′12″S to 35°33′41″S, and 136°32′04″E to 138°00′00″E), is situated to the south of Saint Vincent Gulf, 112 km southwest of Adelaide.

Data processing

Google Earth Engine (GEE), a cloud-based computing platform, facilitated the selection, pre-processing, and downloading of Landsat 8 Surface Reflectance Tier 1 imagery. The study period for the fire was from October 2019 to February 2020. GEE was utilized to integrate all Landsat 8 Surface Reflectance Tier 1 images between June 1, 2019, and October 30, 2019, for pre-fire analysis, and between February 1, 2020, and May 30, 2020, for post-fire analysis, with cloud removal applied.

NASA Shuttle Radar Topography Mission (SRTM) data, including the 1-arcsecond Digital Elevation Model (DEM) and Digital Surface Model (DSM), were utilized to generate a Normalized Digital Surface Model (nDSM). This nDSM was computed to estimate vegetation height on Kangaroo Island.

Segmentation

In this study, we used the multiresolution segmentation algorithm to segment remotely sensed imagery by merging adjacent pixels or small objects based on spectral and spatial information. This algorithm calculated the minimal increase in defined heterogeneity f at each adjacent image object merging step. If this minimal increase f exceeded the heterogeneity threshold t defined by scale parameter Ψ, merging was terminated, and segmentation results were obtained, equation (1) (Benz *et al*. 2004).

$$f = w_{cl} \cdot \Delta h_{cl} + w_{sh} \cdot \Delta h_{sh} \quad (1)$$

$$w_{cl} \in [0,1], w_{sh} \in [0,1]; while\ w_{cl} + w_{sh} = 1$$

Here, w_{cl} and w_{sh} are the spectral and shape weight parameters specified by the user. Spectral and colour heterogeneity difference Δh_{cl} were calculated as following equation (2) (Benz et al. 2004)and difference in shape heterogeneity Δh_{sh} using equation (3) (Benz *et al*. 2004).

$$\Delta h_{cl} = \sum_c w_c (n_m \cdot \sigma_{c,m} - (n_{Obj1} \cdot \sigma_{c,Obj1} + n_{Obj2} \cdot \sigma_{c,Obj2})) \quad (2)$$

$$\Delta h_{sh} = w_{cmp} \cdot \Delta h_{cmp} + w_{sm} \cdot \Delta h_{sm} \quad (3)$$

Here, n was the number of pixels in object. *Obj1* and *Obj2* represented two smaller image objects for merging process, and m represented the larger image object after merging.

Difference in smooth heterogeneity Δh_{sm} and compactness heterogeneity Δh_{cmp} as equation (4) and (5) (Baatz and Schape, 2000; Benz *et al*. 2004):

$$\Delta h_{sm} = n_m \cdot \frac{l_m}{b_m} - (n_{Obj1} \cdot \frac{l_{Obj1}}{b_{Obj1}} + n_{Obj2} \cdot \frac{l_{Obj2}}{b_{Obj2}}) \quad (4)$$

$$\Delta h_{cmp} = n_m \cdot \frac{l_m}{\sqrt{n_m}} - (n_{Obj1} \cdot \frac{l_{Obj1}}{\sqrt{n_{Obj1}}} + n_{Obj2} \cdot \frac{l_{Obj2}}{\sqrt{n_{Obj2}}}) \quad (5)$$

Here, l *is the* perimeter of object and b is perimeter of object's bounding box.

Results and Classifications

All bands or layers were equally weighted for multiresolution segmentation. We evaluated various parameters and criteria, with Figures 1(a)–(c) illustrating the MRS segmentation results. Segmented objects exhibited differences across different data combinations while maintaining the same scale parameter and homogeneity criterion composition.

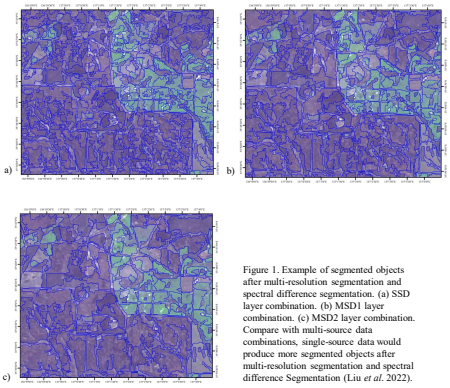

Figure 1. Example of segmented objects after multi-resolution segmentation and spectral difference segmentation. (a) SSD layer combination. (b) MSD1 layer combination. (c) MSD2 layer combination. Compare with multi-source data combinations, single-source data would produce more segmented objects after multi-resolution segmentation and spectral difference Segmentation (Liu *et al*. 2022).

Hierarchical classification, utilizing expert-based spectral and shape knowledge, was applied in this study. It allows for the establishment of complex classification rules across various classes in the hierarchy. Spectral and shape characteristics, including Landsat imagery bands, spectral indices, and nDSM, were considered, reflecting contextual relationships within the study area's landscapes. Fuzzy classification using membership functions and thresholds classification with class descriptions were both utilized. To define membership functions, new expressions were created for each class. A strict trial-and-error approach was necessary to ensure classification accuracy.

Figures 2(a)–(c) display the classification results of segmented imagery, depicting three fire severity levels and five unburned classes: (1) Water Bodies; (2) Buildings & Bare lands; (3) Undisturbed Farmlands & Grasslands; (4) Cleared Farmland; and (5) Unburned Woodlands and Forests. Overall, the classification results of the three different layer combinations exhibit visual similarity on a large scale. The wildfires of 2019–2020 on Kangaroo Island are predominantly located in the western part of the study area, with most burned areas situated in Flinders Chase National Park. However, some burned areas are dispersed throughout the middle of the island due to the wildfire spreading into agricultural and plantation forestry areas.

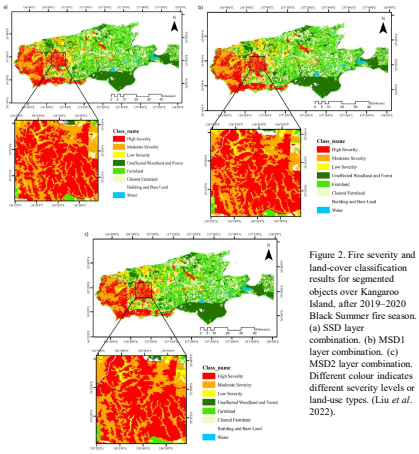

Figure 2. Fire severity and land-cover classification results for segmented objects over Kangaroo Island, after 2019–2020 Black Summer fire season. (a) SSD layer combination. (b) MSD1 layer combination. (c) MSD2 layer combination. Different colour indicates different severity levels or land-use types. (Liu *et al*. 2022).

McNemar's test yielded p-values of $2.44 * 10^{-6}$ for MSD2 vs. MSD1 and $1.01 * 10^{-8}$ for MSD2 vs. SSD, indicating significant differences in classification accuracies at the 99% confidence interval. Additionally, the p-value was $6.19 * 10^{-2}$ for MSD1 vs. SSD, suggesting no statistically significant difference in accuracy at the 95% confidence interval, yet still significant at the 90% confidence interval. Overall, MSD2 segments exhibited higher accuracy compared to MSD1 and SSD, implying that incorporating relevant vegetation indices and multi-source data can enhance classification accuracy.

The pixel values of fire indices were extracted from classified burned areas and subjected to statistical analysis. PostNBR, dNBR, and RdNBR indices exhibited significant differences across fire severities in the segments classifications. This suggests that our object-based image analysis method effectively classifies various fire severity levels, with statistically significant classification results.

In terms of accuracy, the Landsat 8's 30 m resolution led to mixed pixels in built-up areas, misclassifying buildings. However, our method performed well for vegetated or burned areas across all three layer combinations. MSD2 achieved the highest accuracy at 90.2% and a Kappa coefficient of 0.852. SSD achieved an acceptable accuracy of 87.4%. Even with limited data, single-dataset segmentation provided insights into land types and fire severities. Nonetheless, SSD lacked detail and smoothness at burned area edges, limiting its suitability for small-scale bushfire scenarios.

References

Benz UC, Hofmann P, Willhauck G, Lingenfelder I, Heynen M. 2004. Multi-resolution, object-oriented fuzzy analysis of remote sensing data for GIS-ready information. ISPRS J Photogramm Remote Sens. 58(3-4):239-258.

Baatz M, Schape A. 2000. Multi resolution segmentation: an optimum approach for high quality multi scale image segmentation. In Strobl J, Blaschke T, Griesebner G, editors, Angewandte Geographische Informationsverarbeitung. Heidelberg: Wichmann-Verlag; p. 12-23.

Liu J, Freudenberger D, Lim S. 2022. Mapping Burned Areas and Land-Uses in Kangaroo Island Using an Object-Based Image Classification Framework and Landsat 8 Imagery from Google Earth Engine. Geomatics, Natural Hazards and Risk. 13(1):1867-1897.

Further information

For additional information scan the QR code or contact:

Jiyu Liu, PhD Candidate, UNSW Sydney
Jiyu.Liu@unsw.edu.au

Australian Government

UNSW SYDNEY